



Assessing the Seismic Performance of Bridges in Metro Vancouver, BC Using a Simplified Modeling Approach

Anqi Shen¹, Kiranjot Kaur² and Carlos Molina Hutt^{3*}

¹MASc Student, Department of Civil Engineering, University of British Columbia, Vancouver, BC, Canada

²PhD Student, Department of Civil Engineering, University of British Columbia, Vancouver, BC, Canada

³Assistant Professor, Department of Civil Engineering, University of British Columbia, Vancouver, BC, Canada

*carlos.molinahutt@civil.ubc.ca (Corresponding Author)

ABSTRACT

As part of a broader project intended to examine the seismic resilience of the transportation network in Metro Vancouver, BC, this paper proposes a method to evaluate the seismic performance of bridges by means of a simplified analysis procedure. To this end, an inventory of 206 bridges in the region was assembled. As-built drawings for all bridges were reviewed to collect general information, and detailed information for 78 bridges with RC circular columns and rectangular walls was collected, including data for the following parameters: site coordinates, municipality, construction year, code year, material strength, superstructure type, number of spans, span lengths, deck width, number of piers, pier cap weight, number and length of columns or walls, and reinforcement layout for typical piers (i.e., cross section geometry, clear cover, transverse and longitudinal steel). This information was used to inform the development of Single-Degree-of-Freedom (SDOF) models to characterize bridge response by following five key steps: (1) determination of bridge weight, (2) estimation of bridge stiffness, (3) evaluation of lateral strength, (4) definition of a material model to characterize nonlinear response, and (5) SDOF model assembly with the corresponding weight, stiffness, strength and calibrated material model to simulate the force-deformation behavior of the bridge. To illustrate the methodology, we implement it to evaluate the seismic response of a bridge constructed in the 1950s under a hypothetical magnitude-9 (M9) Cascadia Subduction Zone (CSZ) earthquake scenario. The response of a bridge with equivalent strength and stiffness, but modern construction detailing is also evaluated to showcase the difference in expected behavior. The results suggest that the 1950s bridge will experience significant damage with ductility demands close to double those of the equivalent modern bridge.

Keywords: seismic resilience, transportation network, bridge vulnerability, Cascadia Subduction Zone, bridge model

INTRODUCTION

The Cascadia Subduction Zone (CSZ), which is located approximately 120 km from Metro Vancouver, is capable of producing M9 earthquakes with an estimated probability of occurrence of 10-14% within the next 50 years [1]. Previous records have revealed that subduction zone earthquakes are characterized by long durations and high spectral acceleration [1]. The Metro Vancouver region is at a high risk of severe damage resulting from an M9 CSZ earthquake due to its location above the Georgia sedimentary basin, which can further amplify ground motion shaking intensity, something not explicitly considered in Canada's National Seismic Hazard Model or the National Building Code of Canada [2][3]. Due to a lack of quantitative observations of ground shaking during such events, this study leverages a suite of 30 synthetic seismograms of M9 CSZ ground motions developed by the United States Geological Survey (USGS) and the University of Washington (UW) to examine the effects of a major regional earthquake on bridge structural performance [4][5][6], with explicit consideration of sedimentary basin effects. A simplified modeling framework with idealized single-degree-of-freedom (SDOF) oscillators is proposed to assess bridge structural performance. The framework is adapted from the method proposed by Kortum et al. [7], which was used to evaluate the performance of bridges with reinforced concrete (RC) circular columns (Figure 1a) in Washington State. The methodology outlined here includes necessary modifications to enable the application of the framework to the bridge inventory in Metro Vancouver, as well as additional assumptions to include bridges supported by RC rectangular wall piers (Figure 1b). The analysis results, when applied to the broader bridge inventory, can be used to inform prioritization of retrofitting efforts, recovery planning, and future transportation network assessments. The following sections provide an overview of the proposed

analysis methodology, present key assumptions and limitations, and showcase sample calculations and simulation results under a plausible M9 CSZ earthquake scenario.



Figure 1. Sample bridges in Metro Vancouver with: (a) RC circular columns, (b) RC rectangular walls [8].

METHODOLOGY: SIMPLIFIED MODELING FRAMEWORK

The overall methodology involves developing simplified models to characterize the seismic response of bridges. An inventory of bridges was assembled based on data from project partners including the BC Ministry of Transportation and Infrastructure, TransLink and municipalities such as Burnaby, Coquitlam, Delta, Langley City, Langley Township, Port Moody, Surrey, Vancouver and West Vancouver. As-built drawings were reviewed to collect the following parameters: location coordinates, municipality, year built, code year, material strength, superstructure type, span lengths, number of spans, deck width, substructure type, number of piers, pier cap weight, number of columns or walls, length of columns or walls, reinforcement layout (i.e. cross section geometry, clear cover, transverse and longitudinal steel).

Relevant information within the inventory was used to inform the development of simplified bridge models. The development of the simplified models consists of the following key steps, described in more detail in the following subsections:

- 1) Determination of bridge weight;
- 2) Estimation of bridge stiffness;
- 3) Evaluation of lateral strength by performing moment-curvature analysis;
- 4) Definition of a material model, namely the Modified Ibarra Medina Krawinkler Deterioration Model [9] to characterize seismic response including the effects of cyclic deterioration; and
- 5) Development of an SDOF model, with the corresponding weight, stiffness, strength and calibrated material model to characterized nonlinear response in order to simulate the force deformation behavior of the bridge.

Weight Estimation

The present study adopts an SDOF model, in which the weight is assumed to be lumped at the top of the structure. Accordingly, the total weight of the bridges is calculated by excluding half of the weight of the columns or walls, as well as the weight of the foundation as illustrated in Figure 2.

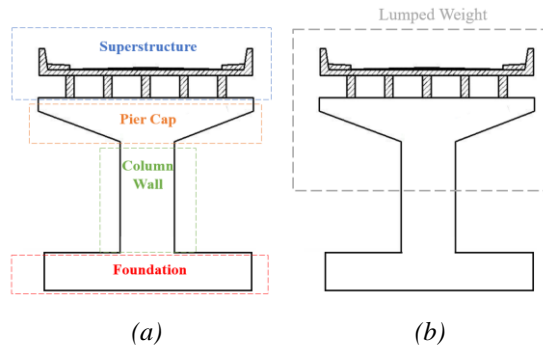


Figure 2. Sketch of (a) bridge components, (b) assumed lumped weight within simplified model.

In order to estimate the weight of the superstructure (i.e., girders, deck, sidewalks and parapets), a set of linear equations are developed based on five representative bridges for each common type of superstructure (i.e., steel girder, prestressed concrete

I-girder, and prestressed concrete box girder). The inventory of steel girder bridges is found to comprise a total of five bridges. In order to maintain consistency in the analysis, five bridges were also selected for the other two bridge types. Supplementary checks were conducted on additional bridges, and it was observed that the equations are good predictors of superstructure weight. These bridges were selected based on a range of ages and span lengths to account for variability in bridge characteristics. Assuming a unit weight of 24kN/m³ for concrete and 77kN/m³ for steel, the normalized weight (i.e., superstructure weight/deck area) is fitted as a function of the longest span length, since longer spans typically require deeper and heavier structural members. This approach enables the estimation of the superstructure weight without requiring a detailed review of drawings for every bridge.

The equations for estimating superstructure weight are presented as Eq. (1) to (3). W_{norm} (kN/m²) is the superstructure weight normalized by deck area. L_{span} (m) is the longest span length.

$$\text{Steel Girder: } W_{norm} = 0.073 \times L_{span} + 3.6412 \quad (1)$$

$$\text{Prestressed Concrete I Girder: } W_{norm} = 0.0923 \times L_{span} + 8.6934 \quad (2)$$

$$\text{Prestressed Concrete Box Girder: } W_{norm} = 0.145 \times L_{span} + 8.9454 \quad (3)$$

Pier Weighted Factor and Effective Length

To determine the total stiffness and strength of the bridges, it is necessary to understand the contribution of each column or wall. However, calculating the properties of each column or wall can be a complex and time-consuming process. To address this, Kortum et al. [7] introduced a weighted factor, alpha (α), to estimate the overall stiffness and strength based on the information of the shortest and longest column. Alpha represents the proportion of columns that can be treated as the shortest column ($0 < \alpha < 1$). For example, an α of 0.5 implies that half of the columns will have the properties of the shortest column. Kortum et al. [7] calibrated α based on a database of more than 200 bridges in Washington State. Their results indicated α values of 0.5, 0.4 and 0.33 for bridges with 2, 3 and 4+ piers, respectively [7]. The same calibration process is applied to the bridge inventory of Metro Vancouver.

The effective length (L_{eff}) is the pier length required for a bridge with equal-length piers to maintain the same lateral stiffness as a bridge with piers of varying length. In this study, the term ‘‘pier’’ may refer to a collection of columns or walls when more than one is present in a line of support. For instance, referring back to Figure 1a, each pier consists of six columns. The pier length is calculated as the average height of columns or walls of each pier, assuming equal column or wall heights within each pier, after verifying that these heights do not vary significantly in the bridge inventory. For each bridge, L_{eff} can be calculated as shown in Eq. (4).

$$\frac{1}{L_{eff}^3} = \frac{1}{numPiers} \sum \frac{1}{L_i^3} \quad (4)$$

L_i is the length of i^{th} pier and numPiers is the number of piers. The effective length can be predicted using α and the shortest and longest length of pier. The $L_{eff, predicted}$ can be expressed as Eq. (5).

$$\frac{1}{L_{eff, predicted}^3} = \frac{\alpha}{L_{short}^3} + \frac{(1-\alpha)}{L_{long}^3} \quad (5)$$

For instance, consider a bridge with two piers, L_{eff} equals to $L_{eff, predicted}$ when alpha equals 0.5. To calibrate alpha for bridges with three and four or more piers, a total of 37 bridges were included in the analysis. For bridges with RC circular columns, α values of 0.5, 0.39 and 0.36 were estimated for bridges with 2, 3 and 4+ piers, respectively. These values are similar to the calibration results of Kortum et al. [7]. With respect to bridges featuring RC rectangular walls, the available database is relatively limited. Therefore, a singular value of α was calibrated for bridge configurations comprising three or more piers, resulting in a value of 0.48. Figure 3 shows the fit between L_{eff} and $L_{eff, predicted}$ for bridges with RC circular columns. Figure 4 shows the same results for bridges with RC rectangular walls.

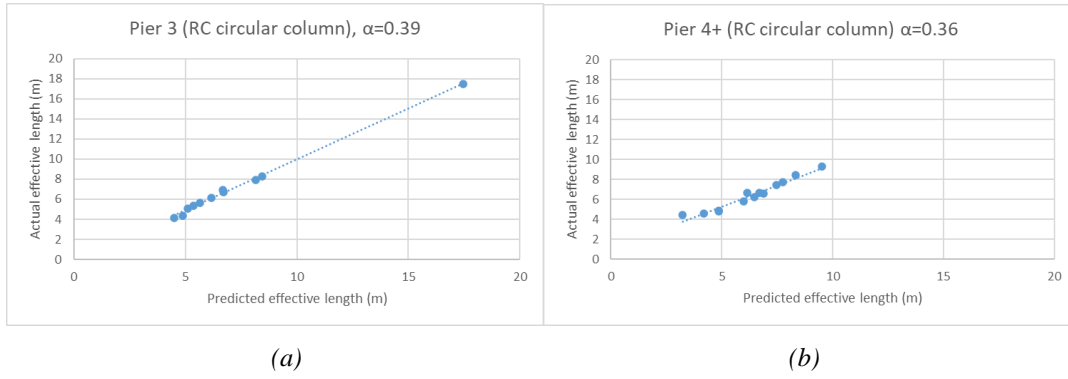


Figure 3. Fit between actual and predicted effective length for bridges with RC circular columns of (a) 3 piers, (b) 4 or more piers.

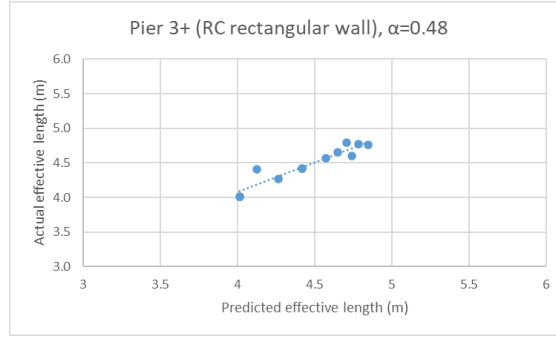


Figure 4. Fit between actual and predicted effective length for bridges with RC rectangular walls.

The total stiffness and strength of the bridge can be estimated using Eq. (6) and (7), which incorporate the weighted factor, α .

$$\text{Stiffness: } K_{bridge} = numCW \cdot [\alpha \cdot K_{short} + (1 - \alpha) \cdot K_{long}] \quad (6)$$

$$\text{Strength: } F_{y,bridge} = numCW \cdot [\alpha \cdot F_{y,short} + (1 - \alpha) \cdot F_{y,long}] \quad (7)$$

K_{bridge} and $F_{y,bridge}$ represent the total bridge stiffness and strength, respectively. K_{short} and $F_{y,short}$ represent the properties of the shortest column or wall, while K_{long} and $F_{y,long}$ represent the properties of the longest column or wall. NumCW is the total number of columns or walls.

Stiffness Estimation

This section provides the stiffness equations for circular and rectangular piers. The effective stiffness ($EI_{eff,cal}$) of circular columns follows the equation proposed by Elwood and Eberhard [10]. It accounts for deformations due to flexure, shear and anchorage slip [10] as shown in Eq. (8):

$$\frac{EI_{eff,cal}}{EI_g} = \frac{0.45 + 2.5P/(A_g f'c)}{1 + 110(\frac{d_b}{D})(\frac{D}{a})} \leq 1.0 \text{ and } \geq 0.2 \quad (8)$$

P is the column axial load, determined by assuming the abutments take the load corresponding to half of the outer spans and the rest of the load is evenly distributed to each column in the pier. E is the elastic modulus which is calculated according to Clause 8.4.1.7 in CSA-S6-14 [11]. A_g is the gross area of the column cross section, I_g is the gross moment of inertia, $f'c$ is the specified concrete compressive strength, d_b is the diameter of longitudinal steel bar, a is shear span and D is the column diameter.

The effective stiffness of rectangular walls can be estimated using the equation proposed by Elwood et al. [12], which considers the effect of compressive axial load and is based on a comprehensive database of rectangular column tests [13]. This equation has been included in the ASCE/SEI 41-13, Seismic Evaluation and Retrofit of Existing Buildings [14]. The flexural rigidity can be expressed as shown in Eq. (9):

$$\frac{E_{eff,cal}}{E I_g} = 0.3 + \left(\frac{P}{A_g f'_c} - 0.1 \right) \leq 0.7 \text{ and } \geq 0.3 \quad (9)$$

A_g represents the gross area of the wall cross section and the remaining parameters are defined in the same way as in Eq. (8). The cross-section geometry of many of the rectangular bridge piers in Metro Vancouver vary along the height (i.e., they are trapezoidal in elevation) as previously shown in Figure 1b. To simplify the modeling process, only the bottom cross section located in the plastic hinge region is considered for both stiffness and strength estimation.

The stiffness of a column or wall with a fixed-fixed or fixed-pinned condition can be calculated as $12EI/L^3$ or $3EI/L^3$, respectively, where L is length of column or wall and EI is the effective stiffness calculated using Eq. (8) or (9). The boundary conditions of each column or wall may vary depending on the different bridge direction considered [7]. In the transverse direction, the piers usually have the cap beam and diaphragms that constrain moment (i.e., fixed-fixed), whereas in the longitudinal direction, this restriction is absent (i.e., fixed-pinned). Once the stiffness of the shortest and longest column or wall has been determined, the total bridge stiffness can be estimated using the weighted factor, alpha, and Eq. (6).

Strength Estimation

The strength of the bridge is determined by performing moment curvature analysis in OpenSeesPy. The moment curvature is derived from a fiber-based section analysis for the circular and rectangular cross sections. With regards to material modeling assumptions, the bilinear steel model (*Steel02*) is used with a strain hardening ratio of 1%, as recommended by Berry and Eberhard [15]. Bar buckling and rupture are also taken into consideration by implementing *MinMax Material* and setting corresponding strain limits. The concrete model follows *Concrete04*, where the unconfined expected concrete strength (f'_{co}) is assumed to be 1.3 times the specified strength [16], the corresponding strain is assumed to be 0.002 and the crushing strain of unconfined concrete is 0.004. The concrete tangent modulus of elasticity (E_{ct}), confined concrete strength and corresponding strain follows the equations proposed by Mander et al. [17] and the ultimate compressive concrete strain is calculated as per the recommendation by Paulay and Priestly [18], assumed equal to the strain at which confining reinforcement fractures. For the tensile behavior of concrete, the properties apply to both confined and unconfined concrete. The tensile strength (f_t) equals the rupture modulus of concrete. The ultimate tensile strain (ϵ_{ut}) is equal to $16\epsilon_{cr}$ according to the tension-stiffening curve proposed by Massicotte et al. [19], where the cracking strain (ϵ_{cr}) equals f_t/E_{ct} .

The RC circular cross section follows the recommended discretization by Berry and Eberhard [15] including 20 core transverse subdivisions, 10 core radial subdivisions, 20 cover transverse subdivisions and one cover radial subdivision (Figure 5a). The RC rectangular cross section built in OpenSeesPy consists of *Patch* and *Layer* which represent concrete and steel layers. The section bends about the weak z-axis in the bridge longitudinal direction and bends about the strong y-axis in the bridge transverse direction (Figure 5b). Note that the circular cross section does not differentiate between strong or weak axis. The number of fibers along the length is chosen to be 800mm such that adding more fibers does not significantly alter the obtained results [20]. The rectangular section is confined in only one direction (Figure 5b), resulting in the assumption of unconfined concrete throughout the entire cross section. It is important to acknowledge that the effect of confinement does not impact the yield points, but rather influences the post-yield behavior.

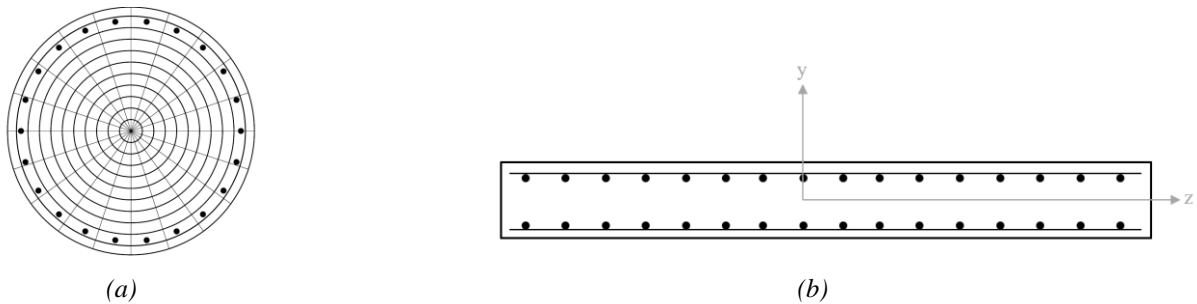


Figure 5. Section layout example of (a) circular section [15], (b) rectangular section.

The effective yield moment (M_y) is derived from the moment curvature curve analysis for each bridge. Numerically, the yield moment is defined as the point at which the slope decreases to 35% of the initial slope. This differs from the conventional yield moment, which refers to the point at which the outer layer of steel begins to yield [21]. In this methodology, the definition of the yield moment aligns with the parameters utilized in the IMK model discussed in the next section.

Figure 6 shows the definitions of M_y . The base shear strength (F_y) is calculated as $2M_y/L$ or M_y/L , depending on the fixed-fixed or fixed-pinned conditions where L is the length of the column or wall. The total base shear strength for the bridge is computed using Eq. (7), which utilizes the alpha factor, along with the strength of the shortest and longest columns or walls.

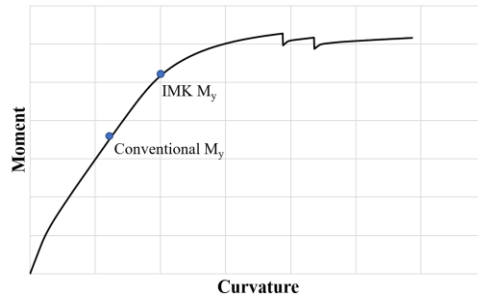


Figure 6. Definitions of M_y .

Modified IMK Model

The SDOF models employ the *Modified Ibarra-Medina-Krawinkler (IMK) Deterioration Model with Peak-Oriented Hysteretic Response* [20] to capture strength and stiffness degradation in the bridges. Figure 7 shows the model behavior and the key parameters.

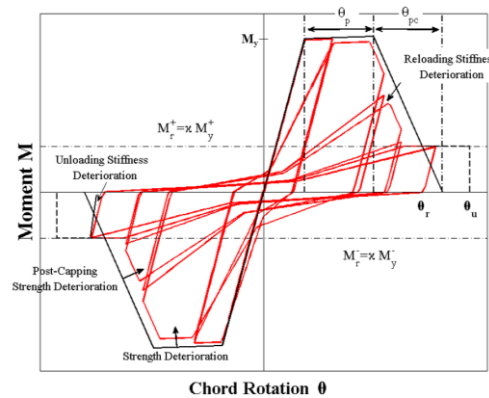


Figure 7. Modified IMK model [9].

During the monotonic loading case, the material has an elastic stiffness (k) up to the yield moment (M_y), i.e., linear elastic response. As the rotation reaches θ_y (M_y/k), the material enters the post-yield region (designated as θ_p), and the stiffness reduces. Subsequently, the material enters the post-capping region (marked as θ_{pc}), in which the material resistance decreases. Beyond that, the material attains its residual strength (M_r) without any further degradation.

In the case of cyclic loading behavior, there are four modes of deterioration including pre-capping strength deterioration, post-capping strength deterioration, unloading stiffness deterioration, and reloading stiffness deterioration. The cyclic deterioration is controlled by the cyclic deterioration parameter, lambda (λ) and the rate of deterioration, c . The value of λ is assumed to remain the same for each mode and c is taken as 1 following the recommendations of Haselton et al. [22].

The above parameters for each bridge can be defined as follows:

- 1) Yield strength (M_y): obtained from moment curvature analysis in OpenSeesPy
- 2) Elastic stiffness (k): determined by effective stiffness equations
- 3) Post yield stiffness (k_p): assumed to be 5% of the elastic stiffness [7]
- 4) Post capping negative tangent stiffness: assumed to be 10% of the elastic stiffness [7]
- 5) Ultimate rotation (θ_u): assumed to be 100 times the sum of θ_y , θ_p , and θ_{pc} [7]
- 6) Residual strength (M_r): assumed to be 1% of yield strength [7]
- 7) Cyclic deterioration parameter (λ): assumed to be the same for all four modes of deterioration [22], calibrated using RC column tests selected from the UW-PEER database [7]
- 8) θ_p : calibrated using RC column tests selected from the UW-PEER database [7]

For the last two parameters that required calibration, Kortum et al. [7] selected 83 column tests from the UW-PEER database to develop the relationship between calibrated parameters and transverse reinforcement ratio (Figure 8). These recommendations are followed in this study.

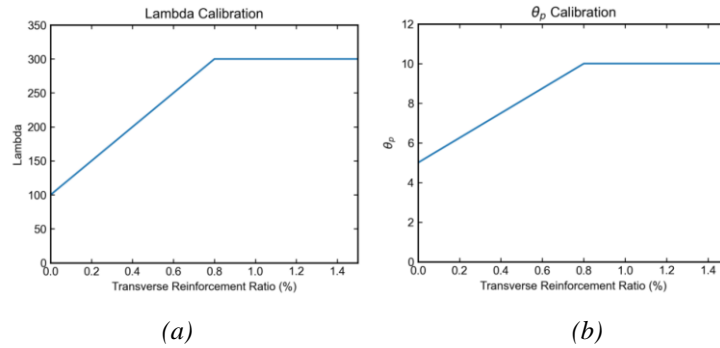


Figure 8. Calibrated parameters (a) λ , (b) θ_p as a function of transverse reinforcement ratio [7].

IMK model parameters lambda and θ_p are set to be representative of two bridge categories: old (pre-1988) and new (1988 to present) to recognize the impact of bridge code evolution in the anticipated seismic performance of bridge structures. The seismic provisions of CSA-S6 Canadian Standards Association bridge codes have evolved over the years. CSA-S6-1966 and 1974 incorporated earthquake load as a function of foundation type and dead load [23][24]. CSA-S6-1978 introduced a seismic zoning map with a 100-year return period [25]. However, it was CSA-S6-1988 that represented a significant change in the hazard level considered in the bridge code, by incorporating a 475-year return period hazard map, i.e., with a probability of exceedance of 10% in 50 years [26]. Consequently, 1988 is designated as the threshold year for defining the age of bridges. Any bridges designed prior to 1988 are classified as older bridges, while those designed according to the code from 1988 to the current standard are defined as newer bridges. Following the recommendations of Kortum et al. [7], we assume that old bridges have a post-yield ductility (D_p/D_y) of 5 and a λ of $100 \times D_y$ whereas the new bridges have a post -yield ductility of 10 and a λ of $300 \times D_y$.

ILLUSTRATIVE EXAMPLE

This section provides an illustrative example of a simplified SDOF model to characterize the response of an old bridge constructed in the 1950s. The results are presented for the bridge in its longitudinal direction by assuming fixed-pinned column boundary condition, which is the controlling case for this example bridge. Table 1 provides relevant bridge information, based primarily on as-built drawings. The response of a new bridge is also simulated by assuming parameters consistent with the old bridge, with the exception of the plastic displacement at peak strength, D_p , and variable lambda, λ , which is the cyclic deterioration parameter that characterizes rate of degradation. While a D_p of $5 \times D_y$ and a λ value of $100 \times D_y$ is assumed for the old bridge, a D_p of $10 \times D_y$ and a λ of $300 \times D_y$ is used for the modern bridge. To account for minimal contributions from the abutments and radiation damping, a 5 percent viscous damping with mass only was assumed in the analysis [7]. Table 2 shows the assumed IMK modeling parameters for both bridges.

Table 1. Sample old bridge information.

Bridge characteristic	Information
Site class	C
Code year	1952 (old)
Year built	1956
Superstructure	prestressed concrete I girder
Substructure	RC piers with circular columns
Total Span(m)	149
Number of spans	7
Columns per pier	2
Total Column Number	12
Foundation	piles
Boundary condition	fixed-pinned
Longitudinal ratio	0.94%
Transverse ratio	0.12% (shortest) / 0.51%(longest)

Table 2. Assumed IMK modeling parameters.

IMK parameters	Assumption	
Yield strength (F_y)	Strength estimation section	
Elastic stiffness (k)	Stiffness estimation section	
Post yield stiffness (k_p)	5% of k	
Yield displacement (D_y)	F_y / k	
Plastic displacement at peak strength (D_p)	$5 \times D_y$ (Old)	$10 \times D_y$ (New)
Lambda (λ)	$100 \times D_y$ (Old)	$300 \times D_y$ (New)
Peak strength (F_{peak})	$F_y + k_p \times D_p$	
Residual strength (F_r)	1% of F_y	
Post capping negative tangent stiffness ratio	10% of k	
Post peak deformation capacity (D_{pc})	$(F_{peak} - F_r) / (0.1 \times k)$	
Deformation at residual strength (D_r)	$D_y + D_p + D_{pc}$	
Ultimate deformation (D_u)	$100 \times D_r$	

A comparison of the moment-curvature analysis of the shortest column in each of the bridges (i.e., old and new) is shown in Figure 9. While the bridges have the same yield moment, yield curvature, and yield base shear strength, the new bridge demonstrates significantly greater ductility. The increased ductility in the moment-curvature analysis is attributed to a larger transverse reinforcement ratio in the new bridge, i.e., 0.51%, in relation to the old bridge, i.e., 0.12%. Nevertheless, this increase in ductility is captured in the IMK model by direct changes to the assumed D_p and λ variables as previously described. The moment-curvature analysis results serve to characterize the total yield base shear strength of the bridge, which can be calculated using Eq. (7) based on α and shortest and longest column strength.

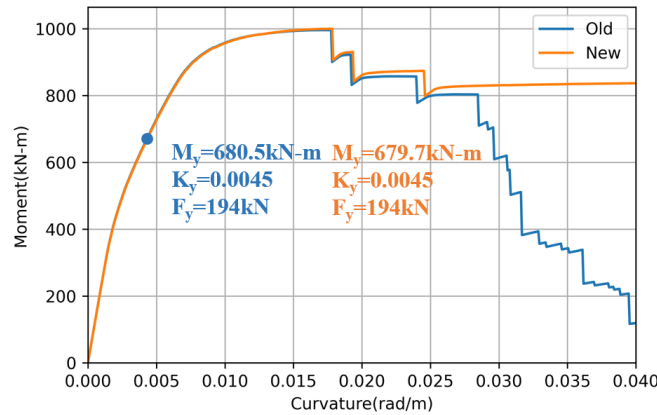


Figure 9. Moment-curvature curve comparison.

These sample bridges are evaluated under one plausible M9 CSZ earthquake scenario. The acceleration time history plot and corresponding response spectrum of the EW ground motion component is shown in Figure 10. Both bridges have a fundamental period of 0.52 second. Figure 11 shows the force-deformation response of the bridges when subjected to the earthquake scenario considered, while Table 3 summarizes the ductility ratios and the corresponding damage state for each bridge. The ductility ratio, defined as the maximum displacement divided by the yield displacement, serves to define the damage state limit in evaluating expected bridge performance. A ductility ratio of between 2 and 3.5 indicates that minimal damage is expected following an earthquake event, with the structure maintaining full-service capabilities. A ductility ratio between 3.5 and 6 suggests moderate damage, which may lead to limited serviceability. A ductility ratio of between 6 and 8 relates to a significant degree of damage, with no expected service. Lastly, a ductility ratio greater than 8 represents complete damage [7]. The results suggest that, under the M9 CSZ earthquake scenario considered, the old bridge will experience significant damage, while the modern bridge will experience moderate damage.

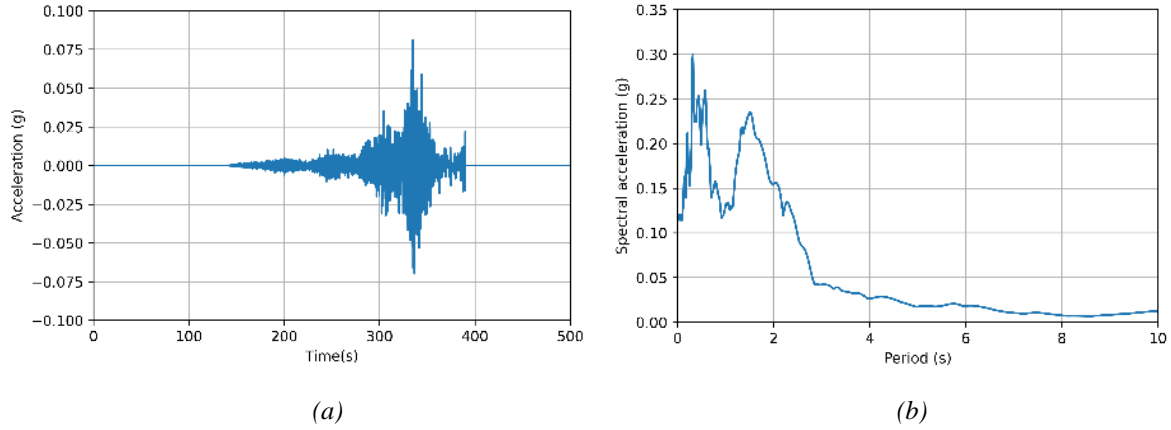


Figure 10. Sample ground motion component: (a) acceleration time history, (b) corresponding response spectrum of a hypothetical M9 CSZ earthquake scenario.

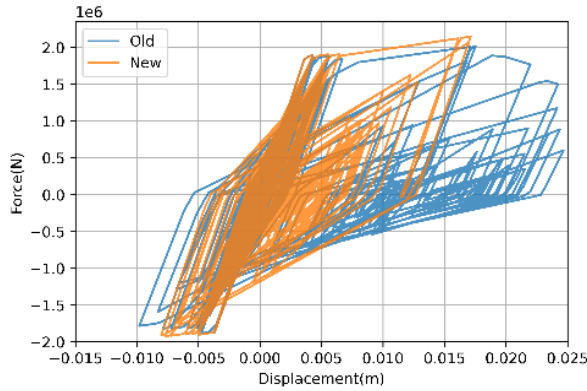


Figure 11. Force-deformation response of the sample bridges.

Table 3. Ductility ratio and damage state of one M9 scenario.

Bridge	Ductility ratio	Damage state
Old	6.69	Significant damage with no expected service
New	4.65	Moderate damage with limited service

CONCLUSIONS

This paper presents a framework to assess the seismic performance of bridges with RC circular columns and rectangular walls using a simplified modeling approach and provides an illustrative example to showcase its implementation to evaluate the response of two bridges in the Metro Vancouver region subjected to a plausible M9 CSZ earthquake scenario. The methodology includes (1) weight calculation, (2) stiffness estimation, (3) lateral strength evaluation, (4) nonlinear response material model definition, and (5) SDOF model assembly with the corresponding weight, stiffness, strength and calibrated material model to simulate the force-deformation behavior of the bridge. The illustrative example compares the performance of an old (1950s) bridge in relation to a comparable new (modern) one. The results suggest that under the earthquake scenario considered, damage to the old bridge will result in significant damage with no expected service, with moderate damage to the new bridge moderate resulting in limited service.

Future work will leverage these simplified models to develop fragility functions for use in a regional seismic risk assessment of the transportation network in Metro Vancouver. While such work will enable rapid regional seismic risk assessments, the simplified model has numerous limitations. Namely, the models neglect (1) the resistance provided by abutments, (2) the impact of bridge skew and curved alignment, and (3) the possibility of span unseating, shear, flexure-shear or foundation failures, any of which could lead to bridge collapse. Future will also expand the modeling approach to account for these important failure modes, and extend the methodology to consider additional types of bridges.

ACKNOWLEDGMENTS

This research was funded by Canada's Natural Sciences and Engineering Research Council under Alliance Grant Number ALLRP 567555-21. We thank our project partners for their assistance in providing structural bridge inventory data for the study (BC MOTI, TransLink, and various Metro Vancouver municipalities). We also express our sincere appreciation to Dr. Marc Eberhard (University of Washington) whose pioneering work on the simplified framework laid the foundation for this study and for providing insights and guidance for this research. We also thank Preetish Kakoty (PhD Candidate, University of British Columbia) for his assistance in obtaining the M9 ground motions for the Metro Vancouver region.

REFERENCES

- [1] Petersen, M. D., Cramer, C. H., and Frankel, A. D. (2002). "Simulations of seismic hazard for the Pacific Northwest of the United States from earthquakes associated with the Cascadia subduction zone." *Pure Appl. Geophys.* 159 (9): 2147–2168. <https://doi.org/10.1007/s00024-002-8728-5>.
- [2] Marafi, N., Eberhard, M.O., Berman, J.W., Wirth, E.A., and Frankel, A.D. (2017). "Effects of deep basins on structural collapse during large subduction earthquakes". *Earthquake Spectra*, 33(3), 963-997.
- [3] Canada, N.B.C. (2015). Associate Committee on the National Building Code, National Research Council of Canada, Ottawa, ON.
- [4] Atwater, B.F., Nelson, A.R., Clague, J.J., Carver, G.A., Yamaguchi, D.K., Bobrowsky, P.T., Bourgeois, J., Darienzo, M.E., Grant, W.C., Hemphill-Haley, E., Kelsey, H.M., Jacoby, G.C., Nishenko, S.P., Palmer, S.P., Peterson, C.D., and Reinhart, M.A. (1995). "Summary of coastal geologic evidence for past great earthquakes at the Cascadia subduction zone". *Earthq. Spectra*, 11(1), 1–18. <https://doi.org/10.1193/1.1585800>.
- [5] Frankel, A.D., Wirth, E.A., Marafi, N., Vidale, J.E., and Stephenson, W.J. (2018). "Broadband synthetic seismograms for magnitude 9 earthquakes on the Cascadia megathrust based on 3D simulations and stochastic synthetics, part 1: Methodology and overall results". *Bull. Seismol. Soc. Am.*, 108(5A), 2347–2369.
- [6] Wirth, E.A., Frankel, A.D., Marafi, N., Vidale, J.E., and Stephenson, W.J. (2018). "Broadband synthetic seismograms for magnitude 9 earthquakes on the Cascadia megathrust based on 3D simulations and stochastic synthetics, part 2: Rupture parameters and variability". *Bull. Seismol. Soc. Am.*, 108(5A), 2370–2388. <https://doi.org/10.1785/0120180029>.
- [7] Kortum, Z, Liu, K.-J., Eberhard, M.O., Berman, J.W., Marafi, N.A., and Maurer, B. (2022). "Impacts of Cascadia subduction zone M9 earthquakes on bridges in Washington State: SDOF idealized bridges," Washington State Department of Transportation report WA-RD 908.1.
- [8] Google Maps. (2023). Street view image of bridges in Metro Vancouver.
- [9] Lignos, D.G., and Krawinkler, H. (2012). "Sidesway collapse of deteriorating structural systems under seismic excitations". Rep.No.TB 177, The John A. Blume Earthquake Engineering Research Center, Stanford University, Stanford, CA.
- [10] Elwood, K. J., and Eberhard, M.O. (2009). "Effective stiffness of reinforced concrete columns". *ACI Structural Journal*, 106(4), 476-484.
- [11] Canadian Standards Association - CSA (2014). *CAN/CSA-S6: Canadian highway bridge design code*. Canada.
- [12] Elwood, K.J., Matamoros, A.B., Wallace, J.W., Lehman, D.E., Heintz, J.A., Mitchell, A.D., Moore, M.A., Valley, M.T., Lowes, L.N., Comartin, C.D., and Moehle, J.P. (2007). "Update to ASCE/SEI 41 concrete provisions". *Earthquake Spectra*, 23(3), 493-523.
- [13] Berry, M.P., Parrish, M., and Eberhard, M.O. (2004). "PEER structural performance database user's manual", Pacific Earthquake Engineering Research Institute, Berkeley, California. Retrieved from <http://nisee.berkeley.edu/spd/>
- [14] ASCE. (2013). *ASCE/SEI 41-13: Seismic Evaluation and Retrofit of Existing Buildings*.
- [15] Berry, M.P., and Eberhard, M.O. (2007). "Performance modeling strategies for modern reinforced concrete bridge columns," PEER-2007/07, Pacific Earthquake Engineering Research Center, University of California, Berkeley.
- [16] Applied Technology Council. (2017). "Guidelines for nonlinear structural analysis for design of buildings." <https://doi.org/10.6028/NIST.GCR.17-917-46v3>
- [17] Mander, J.B., Priestley, M.J.N., and Park, R. (1988). "Theoretical stress-strain model for confined concrete," *Journal of Structural Engineering*, 114(8), 1804-1826.
- [18] Paulay, T., and Priestly, M.J.N. (1992). "Seismic design of reinforced concrete and masonry buildings". New York: Wiley.
- [19] Massicotte, B., Elwi, A.E., and MacGregor, J.G. (1990). "Tension-stiffening model for planar reinforced concrete members," *Journal of Structural Engineering*, 116(11), 3039–3058. [https://doi.org/10.1061/\(ASCE\)0733-9445\(1990\)116:11\(3039\)](https://doi.org/10.1061/(ASCE)0733-9445(1990)116:11(3039)).
- [20] Rinchen, R., Hancock, G., and Rasmussen, K. (2016). "Formulation and implementation of general thin-walled open-section beam-column elements in OpenSees".
- [21] Monti, G., and Petrone, F. (2015). "Yield and ultimate moment and curvature closed-form equations for reinforced concrete sections". *ACI Structural Journal*, 112. <https://doi.org/10.14359/51687747>.

- [22] Haselton, C., Liel, A., Lange, S., and Deierlein, G. (2008). "Beam-column element model calibrated for predicting flexural response leading to global collapse of RC frame buildings". PEER Report 2007/03.
- [23] Canadian Standards Association - CSA (1966). *CAN/CSA-S6: Design of Highway Bridges*, Canada.
- [24] Canadian Standards Association - CSA (1974). *CAN/CSA-S6: Design of Highway Bridges*, Canada.
- [25] Canadian Standards Association - CSA (1978). *CAN3-S6: Design of Highway Bridges*, Canada.
- [26] Canadian Standards Association - CSA (1988). *CAN/CSA-S6: Design of Highway Bridges*, Canada.